^{18}F-FDG PET/MRI Primary Staging of Cervical Cancer: A Pilot Study with PET/CT Comparison

Nghi C. Nguyen[1], Sushil Beriwal[2], Chan-Hong Moon[1], Alessandro Furlan[1], James M. Mountz[1], and Balasubramanya Rangaswamy[1]

[1]Department of Radiology, University of Pittsburgh, Pittsburgh, Pennsylvania; and [2]Department of Radiation Oncology, University of Pittsburgh, Pittsburgh, Pennsylvania

We report our PET/MRI experience from a pilot study that compared the diagnostic performance of ^{18}F-FDG PET/MRI versus PET/CT in staging of cervical cancer. **Methods:** Six adults with newly diagnosed cervical cancer underwent a single ^{18}F-FDG injection with a dual-imaging protocol: standard-of-care PET/CT followed by research PET/MRI. The diagnostic interpretation and SUV_{max} for the 2 modalities were compared. **Results:** Both modalities detected all primary tumors (median size, 3.9 cm) and all 4 metastases present in 2 of the 6 patients (median size, 0.9 cm). PET/MRI provided greater diagnostic confidence than PET/CT and upstaged the disease in 4 patients. On the basis of the imaging findings alone, the additional information from PET/MRI would have led to a change in clinical management in 3 of 6 patients. The primary lesion showed a median SUV of 12.8 on PET/CT and 18.2 on PET/MRI (P = 0.03). SUVs, however, correlated strongly between the 2 modalities (ρ = 0.96, $P < 0.001$). **Conclusion:** Our pilot study supports the notion that PET/MRI has the potential to impact clinical decisions and treatment strategies in women with cervical cancer. Further studies are, however, warranted to define the value that PET/MRI adds to PET/CT.

Key Words: ^{18}F-FDG PET; PET/CT; PET/MRI; cervical cancer; female

J Nucl Med Technol 2020; 48:331–335
DOI: 10.2967/jnmt.120.247080

Gynecologic malignancies are common causes of morbidity and mortality in women (*1*). The International Federation of Gynecology and Obstetrics (FIGO) system is used for staging of most gynecologic malignancies in women (*2*). It is based on the physical examination and a few other procedures such as colposcopy, conization of the cervix, cystoscopy, and rectosigmoidoscopy. A major limitation of FIGO staging is that it lacks locoregional nodal evaluation. Therefore, advanced imaging modalities (CT, MRI, or PET) are often necessary. In this regard, PET/CT with ^{18}F-FDG is a valuable modality for initial staging and restaging of pelvic gynecologic malignancies (*3–7*). Contrast-enhanced MRI is an established imaging modality that has numerous clinical applications due to its superb soft-tissue contrast and lack of ionizing radiation and to its ability to assess cellular density by diffusion-weighted imaging and tissue perfusion by dynamic contrast-enhanced imaging (*6,8,9*). MRI also has the potential to complement the metabolic imaging provided by PET. Therefore, the combination of PET and MRI in an integrated PET/MRI system promises to have a positive impact on disease diagnosis, staging, and restaging. In this article, we report our PET/MRI experience from a pilot study comparing the diagnostic performance of ^{18}F-FDG PET/MRI with standard-of-care (SOC) PET/CT in primary staging of cervical cancer.

MATERIALS AND METHODS

Patient Population

To be included in this pilot study, the patients had to be at least 18 y old, have biopsy-proven pelvic cervical cancer, and be undergoing a SOC ^{18}F-FDG PET/CT examination for initial staging. Patients were excluded if they were pregnant; had significant claustrophobia; had a history of an allergic reaction to gadolinium-based contrast agents; had contraindications to undergoing MRI, including a cardiac pacemaker or metal devices; or had renal insufficiency according to our institutional policy. The study was approved by the Institutional Review Board, and all patients signed an informed-consent form. Six patients were enrolled (median age, 58 y; range, 36–76 y) and underwent a single ^{18}F-FDG injection with a dual-imaging protocol: SOC whole-body PET/CT followed by research pelvic and whole-body PET/MRI. Histopathology at baseline and clinical stage based on FIGO, SOC pelvic MRI, and PET/CT imaging served as the reference standard.

SOC PET/CT

SOC PET/CT of the torso (base of skull to upper thigh) was performed on a Discovery 710 PET/CT scanner (GE Healthcare). The glucose level was less than 200 mg/dL before the ^{18}F-FDG injection. In 2 patients, low-dose, unenhanced CT data (120 kVP, 120 mA, 1.375 pitch) were acquired for attenuation correction and anatomic correlation with PET data. In the remaining patients, diagnostic CT images were obtained for both attenuation correction and diagnostic interpretation, on the basis of institutional guidelines (120 kVP; automatically adjusted amperage; 1.375

Received Apr. 13, 2020; revision accepted May 23, 2020.
For correspondence or reprints contact: Nghi C. Nguyen, UPMC Presbyterian, 200 Lothrop St., East Wing, Suite 200, Pittsburgh, PA 15213.
E-mail: nguyennc@upmc.edu
Published online Jul. 24, 2020.

pitch; intravenous contrast with 100 or 125 mL of iopamidol [Isovue-370; Bracco Diagnostics], dependent on patient weight; oral contrast with 30 mL of diatrizoate meglumine and diatrizoate sodium solution [Gastrografin; Bracco Diagnostics] diluted in 970 mL of water; plus a low-dose, breath-hold CT scan of the chest with 120 kVP and 60 mA). For PET scanning, the injected dose and scan durations were based on institutional guidelines (370 MBq and 2 min/bed position acquisition for a body weight $<$ 55 kg; 444 MBq and 2.5 min/bed position for 56–90 kg; 518 MBq and 3.0 min/bed position for 91–127 kg; and 592 MBq and 3.0 min/bed position for $\geq$128 kg), with a 60-min uptake time. PET images were reconstructed using the standard VUE Point FX algorithm (GE Healthcare), with time-of-flight and ordered-subset expectation maximization, 2 iterations, 32 subsets, and a 6.4-mm gaussian postprocessing filter (*10*). The patients received a median ^{18}F-FDG dose of 477 MBq (range, 396–481 MBq) intravenously.

Research PET/MRI

Research PET/MRI was performed on a Biograph mMR 3T scanner (Siemens Healthcare) (*11*). Glucagon (1 mg intramuscularly) was administered before pelvic imaging to reduce bowel motion artifacts on MRI. Vaginal gel (60 mL) was applied to enhance MRI contrast. Pelvic MRI entailed an unenhanced multiplanar T2-weighted turbo spin-echo sequence, an unenhanced and enhanced T1-weighted Dixon visual background extractor sequence, and diffusion-weighted imaging with b-values or 0 and 700 or 900. Subsequently, whole-body MRI included a non–breath-hold T1-weighted Dixon sequence for attenuation correction (repetition time, 4 ms; first and second echo times, 1 and 2 ms, respectively), an unenhanced T2-weighted half-Fourier acquisition single-shot turbo spin echo sequence, and an enhanced T1-weighted Dixon visual background extractor sequence. A single dose of the gadolinium contrast agent gadobenate dimeglumine (MultiHance [Bracco Diagnostics], 0.1 mmol/kg of body weight) was administered. PET reconstruction was based on ordered-subset expectation maximization with 3 iterations and 21 subsets and a 7-mm gaussian filter. For lesion detection and disease staging, the PET/CT images were read by an experienced nuclear medicine physician with clinical privileges for the interpretation of the diagnostic CT portion, and the PET/MR images were independently read by a dual–board-certified nuclear radiologist. Accuracy and disease stage for each modality were determined in consensus, after a careful review of all imaging findings (PET, diagnostic CT, and MRI). The SUV_{max} of the primary lesion and any suspected metastatic lesions was measured on the whole-body PET scan. The Wilcoxon test was used to compare SUV_{max} between the 2 modalities, and the Spearman coefficient (ρ) was used for SUV_{max} correlation.

RESULTS

The research PET/MRI examination was started with a median delay of 105 min (range, 84–115 min) after the SOC PET/CT examination. This long delay was attributed to the distance and transport between the SOC PET/CT and research PET/MRI facilities. The median time of PET/MRI examination was 69 min (range, 43–78 min). The PET portion for PET/MRI (median, 4.0 min/bed position; range, 3.0–5.0 min) was longer than that for PET/CT (2.5 min/bed position; range, 2.0–2.5 min). The whole-body PET images for PET/MRI were of low count but still useful for interpretation in 3 of the 6 patients, despite the considerable examination delay (close to 2 h). However, the longer pelvic PET images for PET/MRI ($>$10 min/bed position) were of high quality for diagnostic interpretation. Another challenge was misregistration of PET and MR images of the lower chest and upper abdomen due to free breathing during data acquisition. Image artifacts, however, did not affect the pelvic region.

All primary tumors (median, 3.9 cm; range, 2.4–5.2 cm) were detected with both modalities. All 4 suspected nodal or distant metastases (median, 0.9 cm; range, 0.8–1.1 cm), present in 2 of the 6 patients, were detected with both modalities. No change in disease staging occurred in 2 of the 6 patients (33%). However, PET/MRI provided greater diagnostic confidence and accuracy in disease staging and, in 4 of the 6 (67%) patients, was associated with a higher rate for detecting parametrial and peritoneal disease, which was not seen on PET/CT (Table 1). In 1 patient, the upstaging at PET/MRI was minor and would not have resulted in a change in clinical management (patient 3). On the basis of the imaging results only, PET/MRI would have led to a change in clinical management in 3 of the 6 patients (50%). In 2 of these 3 patients, the disease stage was IB on PET/CT (patients 4 and 5) and IIB on PET/MRI. But because they were deemed to have FIGO stage IIB disease, both patients underwent concurrent chemoradiation instead of radical hysterectomy with pelvic nodal dissection. This clinical decision would be consistent with that based on the PET/MRI results. The imaging findings for patient 5 are summarized in Figure 1. In the remaining patient, the disease stage was IIB on PET/CT, which would entail chemotherapy with concurrent pelvic radiotherapy and intracavitary brachytherapy. The disease was upstaged to IVB on PET/MRI because of peritoneal disease (patient 6; Fig. 2). But because the FIGO stage was IIIB, the patient underwent chemotherapy with concurrent pelvic radiotherapy and interstitial brachytherapy, which is comparable to the management used for stage IVB disease with peritoneal invasion, as seen on PET/MRI.

The primary lesion had a median SUV_{max} of 12.8 (range, 10.9–26.4) on PET/CT and 18.2 (range, 12.9–33.7) on PET/MRI ($P = 0.03$). Four suspected metastases showed a median SUV_{max} of 4.3 (range, 2.8–7.9) and 4.9 (range, 2.8–10.6) on PET/CT and PET/MRI, respectively ($P = 0.13$). The lesion SUVs (of all primaries and metastases) correlated strongly between the 2 modalities($\rho = 0.96$; $P < 0.001$).

DISCUSSION

In the past 10 y, there has been significant research on the role of PET/MRI in the clinical management of pelvic gynecologic malignancies. In our pilot study, both PET/CT and PET/MRI detected all primary tumors and all 4 metastases suspected in 2 of the 6 patients. However, PET/MRI provided greater diagnostic confidence than PET/CT and upstaged the disease in 4 patients (67%). If only imaging findings were considered for clinical decisions, PET/MRI would have led to a change in clinical management in 3 of the 6 patients (50%). In clinical practice, however, decisions on patient management are based on FIGO staging and on

TABLE 1
Patient Characteristics; Tumor Stage on FIGO, PET/CT, and PET/MRI; and Impact on Clinical Management

Patient no.	Age (y)	FIGO stage	PET/CT stage	PET/MRI stage	Imaging comments	Change in clinical management? (PET/CT vs. PET/MRI)
1	61	IIB (involving vaginal fornix, with suspected parametrial involvement)	IVB (T2A N0 M1)	IVB (T2B N0 M1)	M1, paraaortic LN, on both modalities	No (both IVB); concurrent chemotherapy with cisplatin, EBRT to pelvis, and interstitial brachytherapy
2	55	IIB (extending into parametrium and upper third of vagina)	IIIB (T2A N1 M0)	IIIB (T2B N1 M0)	MRI detection of parametrial involvement, T2B	No (both IIIB); concurrent chemotherapy with cisplatin, pelvic EBRT, and intracavitary brachytherapy
3	76	IIB (involving parametrium, without sidewall involvement)	IIA (T2A N0 M0)	IIB (T2B N0 M0)	MRI detection of parametrial involvement, T2B	No (IIA vs. IIB); concurrent chemotherapy with cisplatin, pelvic EBRT, and intracavitary brachytherapy
4	60	IIB (involving upper third of vagina and parametrium)	IB (T1B N0 M0)	IIB (T2B N0 M0)	MRI detection of parametrial involvement, T2B	Yes; radical hysterectomy with pelvic nodal dissection (IB) vs. concurrent chemotherapy with cisplatin, pelvic EBRT, and intracavitary brachytherapy (IIB)
5	49	IIB (extending into right fornix and right parametrium)	IB (T1B N0 M0)	IIB (T2B N0 M0)	MRI detection of parametrial involvement, T2B	Yes; radical hysterectomy with pelvic nodal dissection (IB) vs. concurrent chemotherapy with cisplatin, pelvic EBRT, and intracavitary brachytherapy (IIB)
6	36	IIIB (involving parametrium with extension to pelvic sidewall)	IIB (T2B N0* M0)	IVB (T2B N0 M1)	MRI detection of peritoneal involvement, M1	Yes; concurrent chemotherapy with cisplatin, pelvic EBRT, and intracavitary brachytherapy (IIB) vs. interstitial brachytherapy (IVB)

*N0 (focal ureter activity falsely denoted as N1 on PET/CT).
EBRT = external-beam radiotherapy.

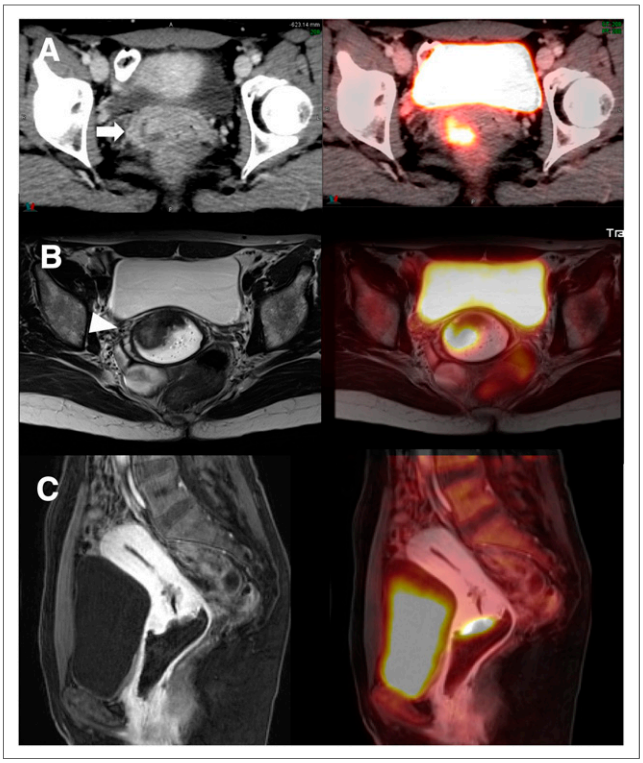

FIGURE 1. A 49-y-old woman with history of poorly differentiated squamous cell carcinoma of cervix, FIGO stage IIB (patient 5). (A) Axial CT (enhanced) (left) and PET/CT (right). (B) Axial MRI (T2-weighted turbo spin-echo, unenhanced) (left) and PET/MRI (T2-weighted turbo spin-echo). (C) Sagittal MRI (T1-weighted Dixon-visual background extractor) (left) and PET/MRI (right), 60 s after gadolinium administration. Primary (arrow) measured 3.5 cm and showed extension into right vaginal fornix (T1B) on PET/CT, with PET/MRI demonstrating additional parametrial involvement (arrowhead; T2B). Disease stage was IB (T1B N0 M0) on PET/CT and IIB (T2B N0 M0) on PET/MRI.

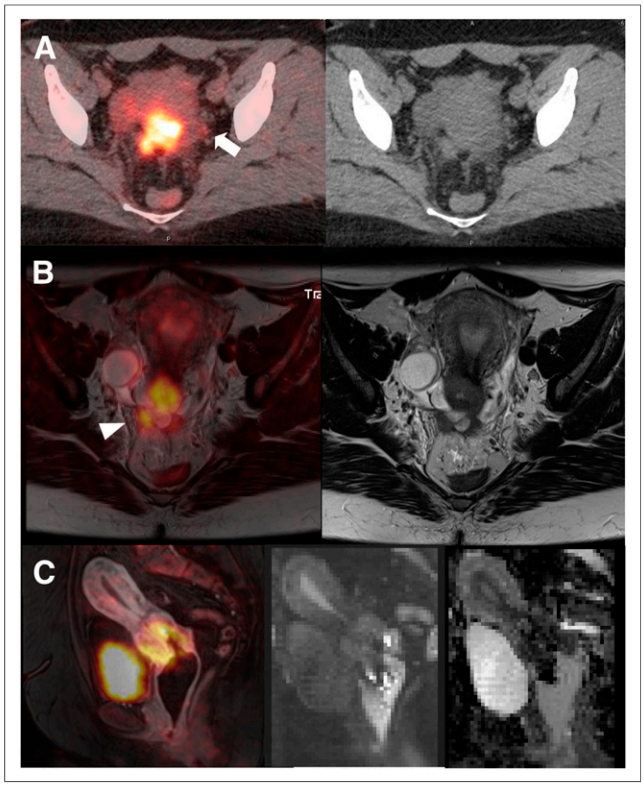

FIGURE 2. A 35-y-old woman with invasive poorly differentiated squamous cell carcinoma of cervix, FIGO stage IIIB (patient 6). (A) Axial PET/CT (unenhanced) (left) and CT (right). (B) Axial PET/MRI (T2-weighted turbo spin-echo) (left) and MRI (right). (C) Sagittal PET/MRI (T1-weighted Dixon–visual background extractor) 60 s after gadolinium enhancement (left), MRI (diffusion-weighted, b700) (middle), and apparent-diffusion-coefficient map (right). ^{18}F-FDG–avid cervical primary, 4.7 cm, is seen well on both PET/CT and PET/MRI. ^{18}F-FDG–avid subcentimeter density in left pelvis on PET/CT (arrow) was thought to be nodal disease (N1), which could not be corroborated on PET/MRI; this finding on PET/CT was most consistent with nonspecific left ureter radioactivity. More importantly, PET/MRI demonstrated peritoneal involvement (M1, arrowhead), which was characterized as parametrial invasion (T2B on CT). Disease stage was IIB (T2B N0 M0) on PET/CT and IVB (T2B N0 M1) on PET/MRI.

corroborative imaging findings such as those from pelvic MRI or ^{18}F-FDG PET/CT. In our cohort, T staging on FIGO showed more advanced tumor infiltration than PET/CT did, but FIGO was compatible with PET/MRI in most cases. As a result, the actual clinical management of the patients did not differ from the management that would have been based on the PET/MRI results.

For cervical cancer staging, current National Comprehensive Cancer Network guidelines recommend imaging (CT, PET/CT, and MRI) for stage IB1 or higher (*12*). Even though image fusion software is available for clinical use, the coregistration of separately acquired MRI data and PET data is often suboptimal, particularly in the body (*13*). Differences in matrix size, imaging plane, and body positioning, as well as other factors related to respiratory motion and physiologic motion of nonrigid structures, can limit an accurate coregistration of the 2 modalities. On the other hand, hybrid PET/MRI provides a precise spatial correlation of data, allowing for an optimal imaging interpretation. More importantly, simultaneous hybrid imaging enables multiparametric PET and MRI measurements, with the potential to provide valuable insight into tumor phenotype and prognostication (*14,15*). PET/MRI is associated with greater diagnostic confidence and accuracy than PET/CT because MRI provides higher soft-tissue contrast than CT. In 4 of our 6 (67%) patients, PET/MRI detected parametrial and peritoneal disease that was missed on PET/CT. Our pilot study affirms the strength of PET/MRI, compared with PET/CT, in diagnostic confidence and accuracy for pelvic staging, as is consistent with previous studies with similar patient populations (*11,16–18*). Because of the upstaging with PET/MRI, 2 patients would have undergone definitive chemoradiation instead of radical hysterectomy with bilateral pelvic lymph node dissection (*12,16,17*).

Grueneisen et al. found that PET/MRI with gadolinium contrast provided correct T staging in 23 of 27 patients (85%) with cervical cancer (*19*). Sensitivity, specificity, and diagnostic accuracy for nodal disease were 91%, 94%, and 93%,

respectively. The results of subsequent studies supported the high diagnostic potential of PET/MRI in cervical cancer staging (*16–18,20*). A recent metaanalysis consisting of 7 studies, with a total of 215 patients for staging and restaging, showed that PET/MRI data provide high diagnostic accuracy in gynecologic malignancies of the pelvis (*21*). On a per-patient basis, the pooled sensitivity and specificity of ^{18}F-FDG PET/MRI were 0.95 (95% confidence interval, 0.86 ± 0.99) and 0.95 (95% confidence interval, 0.74 ± 1.00), respectively. On a lesion basis, the pooled sensitivity and specificity were 0.89 (95% confidence interval, 0.84 ± 0.93) and 0.87 (95% confidence interval, 0.74 ± 0.95), respectively. The overall area under the curve was 0.968 (SE, 0.026).

We acknowledge the limited sample size in our pilot study and the lack of histopathologic confirmation for nodal disease, which limits the generalizability of the results. The SOC PET/CT was undertaken before the research PET/MRI after a single ^{18}F-FDG administration. The time delay between the 2 examinations led to confounding bias concerning the SUV measurements, resulting in higher lesion SUVs as well as higher lesion-to-background SUV ratios on PET/MRI than on PET/CT (*11,18,22*). Nonetheless, the correlation of SUVs remained strong between the 2 modalities. We did not match the PET reconstruction parameters between the 2 modalities (e.g., number of iterations and time-of-flight technique), because our intention was to compare lesion detectability based on the standard image parameters of each scanner.

We did not measure the apparent-diffusion-coefficient values to demonstrate the magnitude of diffusion restriction in our pilot study, as the applied b-values were inconsistent among patients during our effort to optimize diffusion-weighted imaging. Currently, diffusion-weighted imaging is the most important functional MRI application as part of PET/MRI, providing valuable information on tissue cellularity and membrane integrity (*14,15,19,23–27*).

CONCLUSION

Our pilot study supports the notion that PET/MRI provides greater diagnostic confidence and accuracy than PET/CT in the initial staging of cervical cancer. Most importantly, PET/MRI complements FIGO staging and has the potential to impact clinical decisions and treatment strategies. Further studies are warranted to define the added value of PET/MRI to PET/CT.

DISCLOSURE

No potential conflict of interest relevant to this article was reported.

ACKNOWLEDGMENTS

We thank Suzanne Burdin, BS, and Rose Jarosz, BS, for technical support.

REFERENCES

1. Cancer facts and figures: 2018. American Cancer Society website. https://www.cancer.org/content/dam/cancer-org/research/cancer-facts-and-statistics/annual-cancer-facts-and-figures/2018/cancer-facts-and-figures-2018.pdf. Published 2018. Accessed August 19, 2020.
2. Pecorelli S, Zigliani L, Odicino F. Revised FIGO staging for carcinoma of the cervix. *Int J Gynaecol Obstet.* 2009;105:107–108.
3. Atri M, Zhang Z, Dehdashti F, et al. Utility of PET-CT to evaluate retroperitoneal lymph node metastasis in advanced cervical cancer: results of ACRIN6671/GOG0233 trial. *Gynecol Oncol.* 2016;142:413–419.
4. Zhao Q, Feng Y, Mao X, Qie M. Prognostic value of fluorine-18-fluorodeoxyglucose positron emission tomography or PET-computed tomography in cervical cancer: a meta-analysis. *Int J Gynecol Cancer.* 2013;23:1184–1190.
5. Bollineni VR, Ytre-Hauge S, Bollineni-Balabay O, Salvesen HB, Haldorsen IS. High diagnostic value of ^{18}F-FDG PET/CT in endometrial cancer: systematic review and meta-analysis of the literature. *J Nucl Med.* 2016;57:879–885.
6. Tempany CM, Zou KH, Silverman SG, Brown DL, Kurtz AB, McNeil BJ. Staging of advanced ovarian cancer: comparison of imaging modalities—report from the Radiological Diagnostic Oncology Group. *Radiology.* 2000;215:761–767.
7. Gu P, Pan LL, Wu SQ, Sun L, Huang G. CA 125, PET alone, PET-CT, CT and MRI in diagnosing recurrent ovarian carcinoma: a systematic review and meta-analysis. *Eur J Radiol.* 2009;71:164–174.
8. Sala E, Wakely S, Senior E, Lomas D. MRI of malignant neoplasms of the uterine corpus and cervix. *AJR.* 2007;188:1577–1587.
9. Frei KA, Kinkel K, Bonel HM, Lu Y, Zaloudek C, Hricak H. Prediction of deep myometrial invasion in patients with endometrial cancer: clinical utility of contrast-enhanced MR imaging—a meta-analysis and Bayesian analysis. *Radiology.* 2000;216:444–449.
10. Vandendriessche D, Uribe J, Bertin H, De Geeter F. Performance characteristics of silicon photomultiplier based 15-cm AFOV TOF PET/CT. *EJNMMI Phys.* 2019;6:8.
11. Beiderwellen K, Grueneisen J, Ruhlmann V, et al. [^{18}F]FDG PET/MRI vs. PET/CT for whole-body staging in patients with recurrent malignancies of the female pelvis: initial results. *Eur J Nucl Med Mol Imaging.* 2015;42:56–65.
12. NCCN clinical practice guidelines in oncology: cervical cancer—version 1.2020. National Comprehensive Cancer Network website. https://www.nccn.org/professionals/physician_gls/default.aspx. Published 2020.
13. Judenhofer MS, Cherry SR. Applications for preclinical PET/MRI. *Semin Nucl Med.* 2013;43:19–29.
14. Floberg JM, Fowler KJ, Fuser D, et al. Spatial relationship of 2-deoxy-2-[^{18}F]-fluoro-D-glucose positron emission tomography and magnetic resonance diffusion imaging metrics in cervical cancer. *EJNMMI Res.* 2018;8:52.
15. Pinker K, Andrzejewski P, Baltzer P, et al. Multiparametric [^{18}F]fluorodeoxyglucose/[^{18}F]fluoromisonidazole positron emission tomography/magnetic resonance imaging of locally advanced cervical cancer for the non-invasive detection of tumor heterogeneity: a pilot study. *PLoS One.* 2016;11:e0155333.
16. Queiroz MA, Kubik-Huch RA, Hauser N, et al. PET/MRI and PET/CT in advanced gynaecological tumours: initial experience and comparison. *Eur Radiol.* 2015;25:2222–2230.
17. Schwartz M, Gavane SC, Bou-Ayache J, et al. Feasibility and diagnostic performance of hybrid PET/MRI compared with PET/CT for gynecological malignancies: a prospective pilot study. *Abdom Radiol (NY).* 2018;43:3462–3467.
18. Xin J, Ma Q, Guo Q, et al. PET/MRI with diagnostic MR sequences vs PET/CT in the detection of abdominal and pelvic cancer. *Eur J Radiol.* 2016;85:751–759.
19. Grueneisen J, Schaarschmidt BM, Heubner M, et al. Integrated PET/MRI for whole-body staging of patients with primary cervical cancer: preliminary results. *Eur J Nucl Med Mol Imaging.* 2015;42:1814–1824.
20. Grueneisen J, Beiderwellen K, Heusch P, et al. Correlation of standardized uptake value and apparent diffusion coefficient in integrated whole-body PET/MRI of primary and recurrent cervical cancer. *PLoS One.* 2014;9:e96751.
21. Nie J, Zhang J, Gao J, et al. Diagnostic role of ^{18}F-FDG PET/MRI in patients with gynecological malignancies of the pelvis: a systematic review and meta-analysis. *PLoS One.* 2017;12:e0175401.
22. Grueneisen J, Schaarschmidt BM, Heubner M, et al. Implementation of FAST-PET/MRI for whole-body staging of female patients with recurrent pelvic malignancies: a comparison to PET/CT. *Eur J Radiol.* 2015;84:2097–2102.
23. Grueneisen J, Schaarschmidt BM, Beiderwellen K, et al. Diagnostic value of diffusion-weighted imaging in simultaneous ^{18}F-FDG PET/MR imaging for whole-body staging of women with pelvic malignancies. *J Nucl Med.* 2014;55:1930–1935.
24. Brandmaier P, Purz S, Bremicker K, et al. Simultaneous [^{18}F]FDG-PET/MRI: correlation of apparent diffusion coefficient (ADC) and standardized uptake value (SUV) in primary and recurrent cervical cancer. *PLoS One.* 2015;10:e0141684.
25. Sun H, Xin J, Zhang S, et al. Anatomical and functional volume concordance between FDG PET, and T2 and diffusion-weighted MRI for cervical cancer: a hybrid PET/MR study. *Eur J Nucl Med Mol Imaging.* 2014;41:898–905.
26. Meyer HJ, Purz S, Sabri O, Surov A. Cervical cancer: associations between metabolic parameters and whole lesion histogram analysis derived from simultaneous ^{18}F-FDG-PET/MRI. *Contrast Media Mol Imaging.* 2018;2018:5063285.
27. Olsen JR, Esthappan J, DeWees T, et al. Tumor volume and subvolume concordance between FDG-PET/CT and diffusion-weighted MRI for squamous cell carcinoma of the cervix. *J Magn Reson Imaging.* 2013;37:431–434.